Estimation of Looming from LiDAR

Juan D. Yepes and Daniel Raviv
Florida Atlantic University, Electrical Engineering and Computer Science Department,

Keywords: Looming, Obstacle Avoidance, Collision Free Navigation, LiDAR, Threat Zones, Autonomous Vehicles.

Abstract: Looming, traditionally defined as the relative expansion of objects in the observer's retina, is a fundamental visual cue for perception of threat and can be used to accomplish collision free navigation. The measurement of the looming cue is not only limited to vision and can also be obtained from range sensors like LiDAR (Light Detection and Ranging). In this article we present two methods that process raw LiDAR data to estimate the looming cue. Using looming values, we show how to obtain threat zones for collision avoidance tasks. The methods are general enough to be suitable for any six-degree-of-freedom motion and can be implemented in real-time without the need for fine matching, point-cloud registration, object classification or object segmentation. Quantitative results using the KITTI dataset shows advantages and limitations of the methods.

1 INTRODUCTION

Collision avoidance continues to be one of the greatest challenges in unmanned vehicles (Yasin et al., 2020) and autonomous driving (Roriz et al., 2021), where the demand for increasingly robust, fast and safe systems is crucial for the development of these industries. It is closely tied with the perception of threat. For creatures in nature, this task seems to be more fundamental than the recognition of shapes (Albus and Hong, 1990). Studies in biology have shown strong evidence of neural circuits in the brains of creatures related to the identification of looming (Ache et al., 2019). Basically, creatures have evolved instinctive escaping behaviors that tie perception directly to action (Evans et al., 2018).

The visual looming cue, defined quantitatively by (Raviv, 1992) as the instantaneous change of range over the range, is related to the increase in size of an object projected on the observer's retina. It is an indication of threat that can be used to accomplish collision avoidance tasks. The looming cue is not limited exclusively to vision and can be computed from active sensors like LiDAR (Light Detection and Ranging).

In general, architectures for autonomous vehicles consist of three sub-systems: Perception, Planning and Control (Sharma et al., 2021). The Perception sub-system can be divided subsequently into three categories: camera-based, LiDAR-based and sensor fusion-based approaches (Wang et al., 2018). Traditionally the task of obstacle avoidance is exclusively related to the Planning and Control subsystems (Yasin et al., 2020) where classification of objects is a prerequisite prior to any global or local path planning action (Mujumdar and Padhi, 2011).

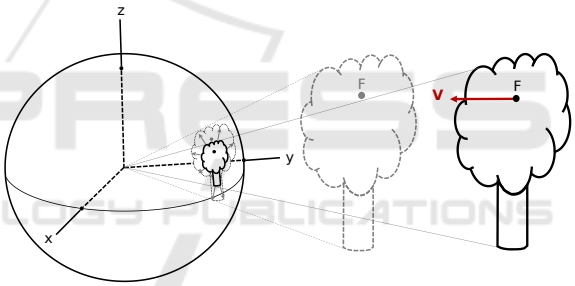

Figure 1: Visualizing looming cue: relative expansion of 3D object on 2D image sensor.

In contrast, it has been shown that obstacle avoidance tasks can be accomplished without 3D reconstruction (structure from motion), using the Active Perception paradigm (Aloimonos, 1992).

In this paper we follow an approach similar to (Raviv and Joarder, 2000). It uses 2D raw data to directly get quantitative indication of visual threat. We present methods for obtaining looming values using raw LiDAR data and threat zones. This allows for real-time collision avoidance tasks without 3D reconstruction or scene understanding. In the proposed approach further processing of the LiDAR point cloud is not required for obtaining threat zones.

Yepes, J. and Raviv, D.
Estimation of Looming from LiDAR.
DOI: 10.5220/0011115300003191
In *Proceedings of the 8th International Conference on Vehicle Technology and Intelligent Transport Systems (VEHITS 2022)*, pages 455-462
ISBN: 978-989-758-573-9; ISSN: 2184-495X

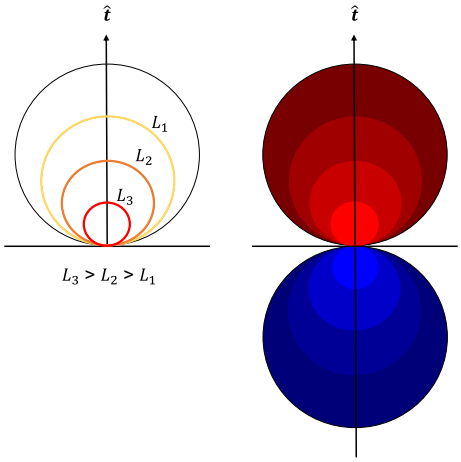

Figure 2: Equal looming spheres as shown in red for $(L > 0)$ and blue for $(L < 0)$.

2 RELATED WORK

2.1 Visual Looming

The visual looming cue is related to the relative change in size of an object projected on the observer's retina as the range to the object varies (Figure 1). It is *quantitatively* defined as the negative value of the time derivative of the range between the observer and a point in 3D divided by the range (Raviv, 1992):

$$L = -\lim_{\Delta t \to 0} \frac{\left(\frac{r_2 - r_1}{\Delta t}\right)}{r_1} = -\left(\frac{\dot{r}}{r}\right) \quad (1)$$

where L denotes looming, dot denotes derivative with respect to time.

2.1.1 Looming Properties

Note that the result for L in equation (1) is a scalar value which is *dependent* on the vehicle translation component but *independent* of the vehicle rotation. It was shown that points in space around the vehicle that share the same looming values form equal looming spheres with centers that lie on the instantaneous translation vector $\mathbf{t}$ and intersect with the vehicle origin. These looming spheres expand and contract depending on the magnitude of the translation vector (Raviv, 1992). Regions for obstacle avoidance and other behavior related tasks can be defined using equal looming surfaces. For example, a high danger zone for $L > L_3$, medium threat for $L_3 > L > L_2$ and low threat for $L_2 > L > L_1$ (Figure 2).

2.1.2 Advantages of Looming

Using the same LiDAR point cloud, it is possible to get looming directly without 3D reconstruction and without knowing the ego-motion of the LiDAR sensor. Looming is measured in $time^{-1}$ units and provide information about imminent threat to the observer. There is no need for scene understanding such as identifying cars, bikes, or pedestrians. In addition, looming provides threats for moving objects as well. Extracting looming for obstacle avoidance using point cloud raw data from LiDAR is the main contribution of this paper.

2.1.3 Measuring Visual Looming

Several methods were shown to quantitatively extract the visual looming cue on a 2D image sequence by measuring attributes like area, brightness, texture density and image blur (Raviv and Joarder, 2000).

The Visual Threat Cue (VTC), just like the visual looming, is a measurable time-based scalar value that provides some measure for a relative change in range between a 3D surface and a moving observer (Kundur and Raviv, 1999).

Event-based cameras were shown to detect looming objects in real-time from optical flow using clustering of pixels (Ridwan, 2018).

2.2 LiDAR for Obstacle Avoidance

In general, collision avoidance approaches require 3D reconstruction of the environment where collision free paths can be computed an executed. Several deep learning and path planning techniques for autonomous driving were mentioned in (Grigorescu et al., 2020). Point clouds, provided by LiDAR sensors, are the preferred representation for many scene understanding related applications. These point clouds are processed to build real-time 3D localization maps, using SLAM (Simultaneous Localization and Mapping) and related techniques (Zhang and Singh, 2014). In general, most methods use 3D object detection, segmentation and scene understanding. In addition, ego-motion is required for obstacle avoidance and autonomous navigation.

In contrast, our approach provides relevant information for the task of collision avoidance in the form of a real-time looming threat map. This allows the direct transition from perception to action without the need of object identification, finding ego-motion or 3D reconstruction.

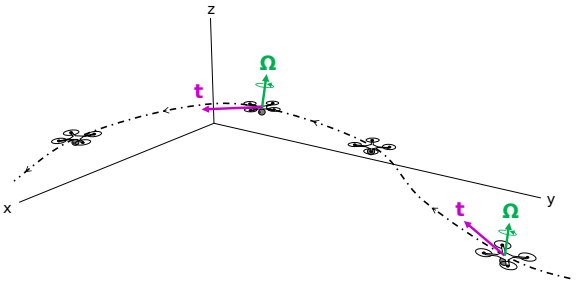

Figure 3: Vehicle undergoing a generalized six-degree-of-freedom motion relative to the *world frame*. **t** is the translation velocity vector, and Ω is the rotation vector.

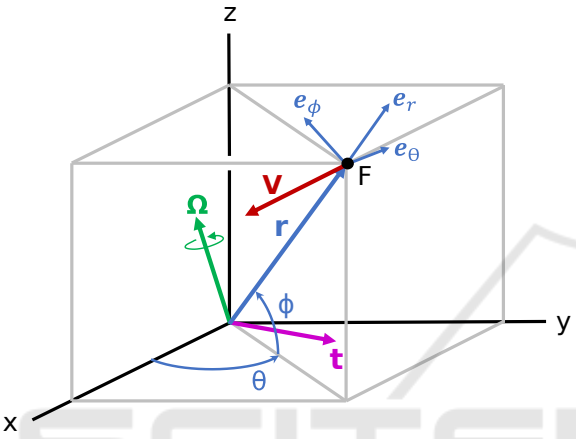

Figure 4: LiDAR coordinate system.

3 METHOD

3.1 Derivation of Looming from the Relative Velocity Field

We will derive a general expression for Looming (L) for any six-degree-of-freedom motion that involves velocity and range using spherical coordinates. Then we can apply this expression with LiDAR data.

Vehicle Motion. Consider a vehicle undergoing a general six-degree-of-freedom motion in a 3-D space relative to an arbitrary stationary reference point.

At any given time, the vehicle will have an associated translation velocity vector **t** and a rotation vector Ω relative to the *world frame* as shown on Figure 3.

LiDAR Coordinate System. Consider a local coordinate system centered at the LiDAR sensor, fixed to the moving vehicle. We chose the x-axis to be aligned with the forward direction of the vehicle and the z-axis to be aligned with the vertical orientation. Refer to Figure 4: In this frame any stationary feature on the 3-D scene can be represented by spherical coordinates (r, θ, ϕ) where r is the radial range to the feature point **F**, θ is the azimuth angle measured from the x-axis and ϕ is the elevation angle from the XY-plane.

Relative Velocity Field. In our analysis the vehicle is undergoing a generalized six-degree-of-freedom motion in the *world frame*. This is equivalent to interpreting the motion as the vehicle being stationary and the feature point **F** moving on the *LiDAR frame* with opposite velocity vector $-\mathbf{t}$ and rotation $-\Omega$.

In this *LiDAR frame* the feature **F** has relative velocity vector:

$$\mathbf{V} = (-\mathbf{t}) + (-\Omega \times \mathbf{r}) \tag{2}$$

We can also conveniently express **V** using spherical unit vector components $\mathbf{e}_r, \mathbf{e}_\theta, \mathbf{e}_\phi$:

$$\mathbf{V} = \dot{r}\mathbf{e}_r + r\dot{\theta}\cos(\phi)\mathbf{e}_\theta + r\dot{\phi}\mathbf{e}_\phi \tag{3}$$

Note that equations (2) and (3) refer to the same *relative velocity field* **V**.(**r** in bold refers to the range vector and the scalar r to its magnitude, i.e $r = |\mathbf{r}|$).

Looming from Normalized Velocity Field. We can get another expression for looming (L) by dividing equations (2) and (3) by r, expanding **t** and Ω, and grouping components by $\mathbf{e}_r$:

$$L = \frac{\mathbf{t} \cdot \mathbf{e}_r}{r} \tag{4}$$

Notice that by knowing the instantaneous translation vector of the vehicle **t** and range r, we can compute the looming value (L) for any point along the directional unit vector $\mathbf{e}_r$.

3.2 Looming from LiDAR

We propose two ways to extract looming from LiDAR data.

3.2.1 Using LiDAR Data Only

Looming can be estimated using LiDAR point clouds. Each full scan of the LiDAR results in a range image grid. Using two consecutive scans we get two range image grids as obtained from the same 3D environment. Theoretically, if the range value of each LiDAR pixel in each grid corresponds to the same 3D point in space, we obtain two range values from which the looming can be estimated, where the only error is due to the range values as obtained from the LiDAR measurements.

However, this is practically not the case: the problem with this approach is that due to the vehicle motion the assumption may hold only when the changes

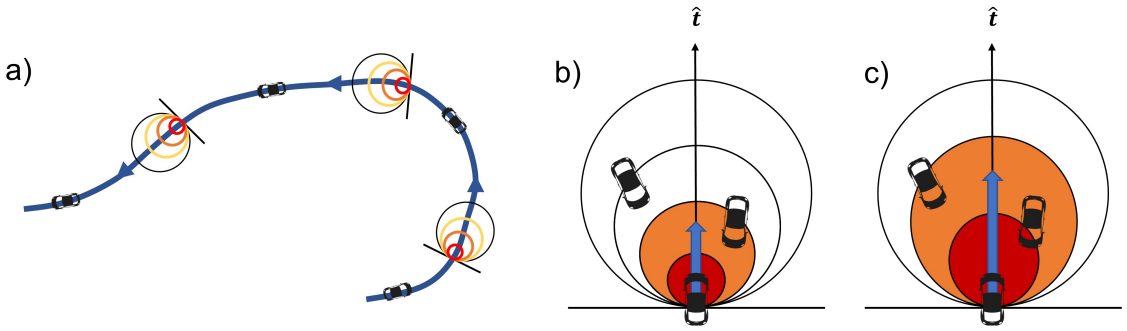

Figure 5: Equal looming circles. a) Vehicle trajectory, b) High and medium threat zones, c) Vehicle motion: higher speeds results in an expansion of the threat region.

from one image to another are infinitesimally small. To minimize the effect of incorrect looming calculations and improve the robustness of the approach, we use interpolation/decimation and discretization of the data in the grid allowing for range values that are closer to the real ones.

Equation (5) shows the specific calculations.

$$L_{ij} = -\frac{\left(\frac{r(\theta_i,\phi_i)_{j+1} - r(\theta_i,\phi_i)_j}{\Delta t}\right)}{r(\theta_i,\phi_i)_{j+1}} \quad (5)$$

where $i = [1,2,..,n]$, n is the number of points on the grid, $j+1, j$ correspond to the current and previous point cloud sample sets. The resulting L_{ij} can be interpreted as a LiDAR-based looming image from where threat zones can be obtained for the purpose of collision avoidance actions.

3.2.2 Using LiDAR + IMU

Another method for obtaining looming is using LiDAR and IMU (Inertial Measurement Unit). Even though this is not the primary focus of this paper, its purpose is to demonstrate that LiDAR combined with IMU increase the robustness of computation of looming. However, this approach has its drawback because it gives incorrect values of looming for moving objects. Note that it requires only the translation vector and not the rotation component of the LiDAR sensor. It uses ego-motion only partially, and there is no need for 3D reconstruction and image understanding.

We can compute looming (L) for every measured stationary point by using equation (4). The range r is provided by the LiDAR sensor for every point on the point cloud. The instantaneous translation vector $\mathbf{t}$ of the vehicle can be obtained from the IMU or by other odometry methods.

For special cases where vehicles have little side motion, like most automotive applications, the translation vector can be assumed to be equal to the vehicle forward motion component, and the magnitude (speed) can be obtained from the vehicle odometer or from the speed encoder of the wheel.

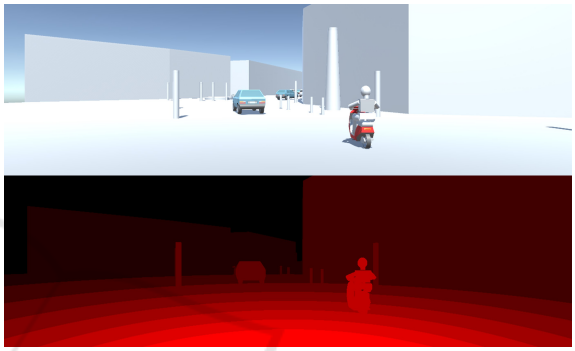

Figure 6: Looming from synthetic data: top image is the scene; bottom image is the looming map (Brighter red represents higher value of looming).

3.2.3 Threat Maps

From either method, threat regions can be obtained from looming values by assigning specific thresholds. For example, *High*, *Medium*, or *Low* threat zones. (Figure 5).

4 RESULTS

We present results of the methods for obtaining looming and threat zones using synthetic and real data.

4.1 Ground Truth Looming with Synthetic Data

A simulation of a moving vehicle in a stationary environment was performed using the Unity3D game engine. In this simulation the vehicle is translating forward at a constant speed between some stationary objects. The top part of Figure 6 shows an actual image of the scene. The bottom part of Figure 6 shows

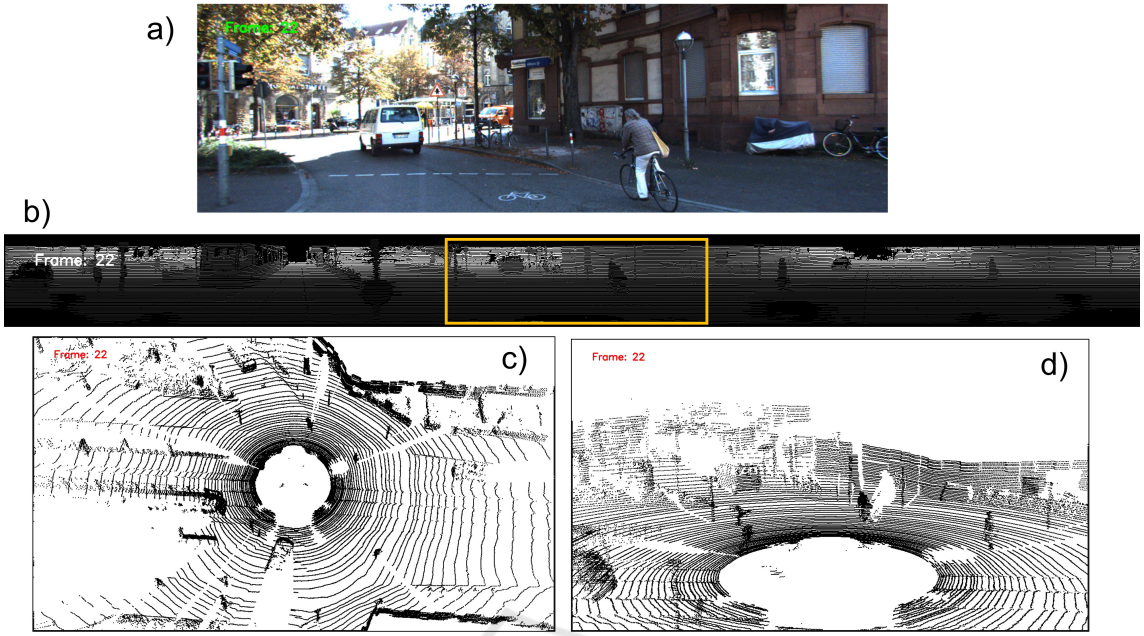

Figure 7: LiDAR data from the KITTI dataset: a) Original image from a color camera mounted on the vehicle, b) 360 degrees LiDAR data, the yellow rectangle corresponds to the color camera field of view, c) Top view of point cloud in 3D, d) Bird's eye 3D view of point cloud.

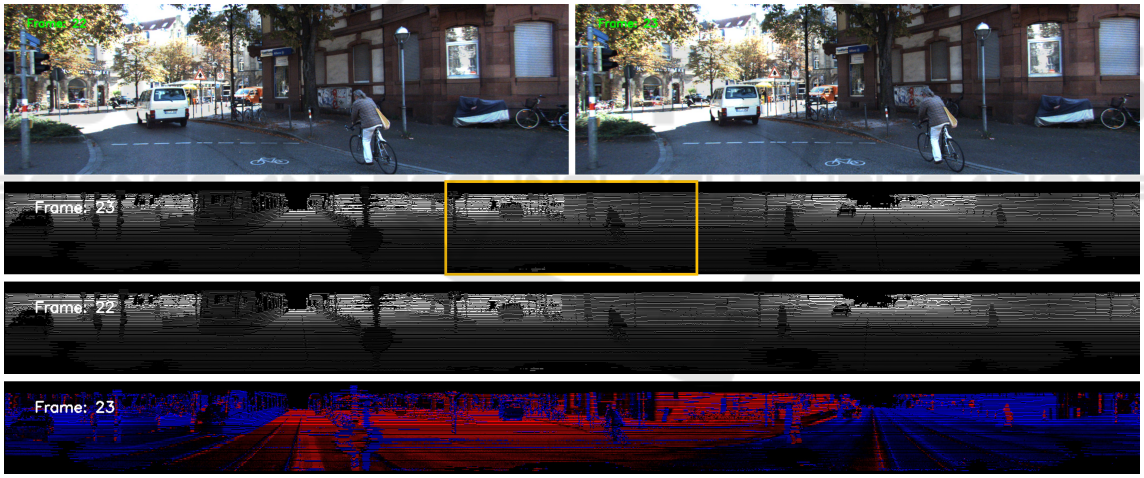

Figure 8: Estimated looming from LiDAR only. (Refer to text for details).

ground truth looming computed using equation (1) and shown from the observer point of view. A pixel shader filter was implemented to visualize the looming value as levels of red color. Brighter red color corresponds to higher value of looming.

4.2 LiDAR Data from KITTI Dataset

We processed real data using a particular city drive from the well-known KITTI dataset (Geiger et al., 2013). The KITTI dataset includes raw data provided by a Velodyne 3D laser scanner (LiDAR) along with velocity vector from a GPS/IMU inertial navigation system. Color camera images were only used as reference as shown in Figure 7.a. The LiDAR sensor specifications are: Velodyne HDL-64E rotating 3D laser scanner, 10 Hz, 64 beams, 0.09-degree angular resolution, 2 cm distance, accuracy, provides around 1.3 million points/second, field of view: 360 degrees horizontal, 26.8 degrees vertical, range:120 m.

Shown in Figure 7 are the original images from one of the vehicle color cameras and gray-scale representations of the raw LiDAR data. A yellow rectangle indicates where the LiDAR data matches the field

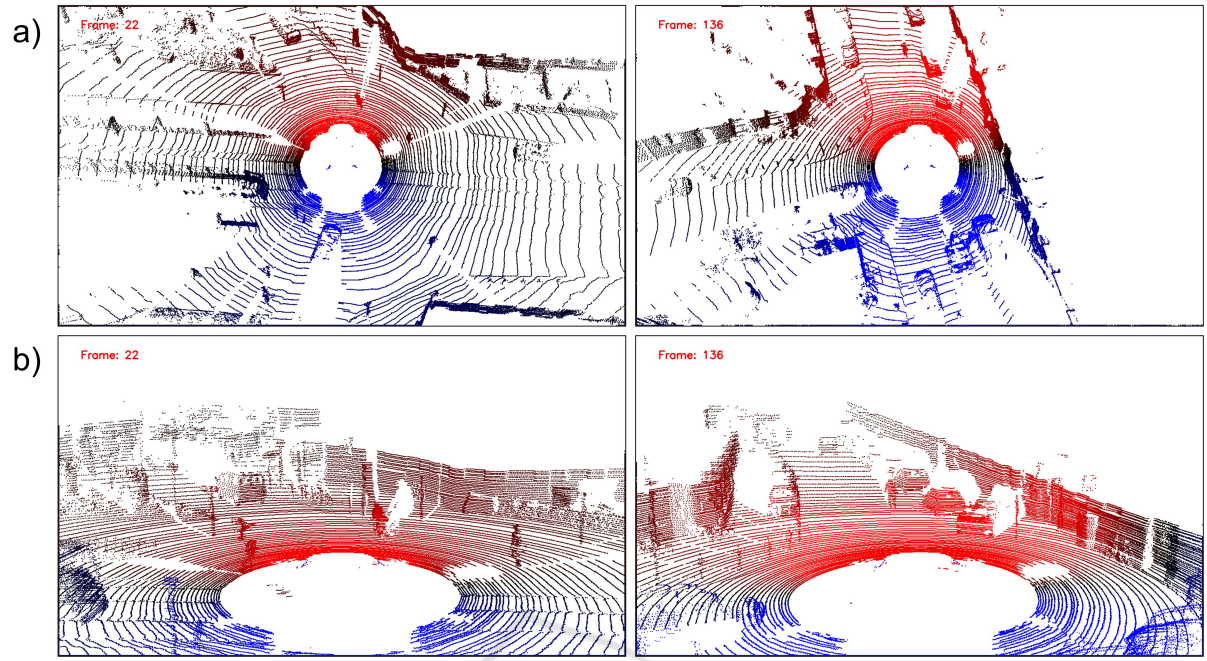

Figure 9: Looming from LiDAR (red is potential threat): a) Top view, b) Bird's eye view.

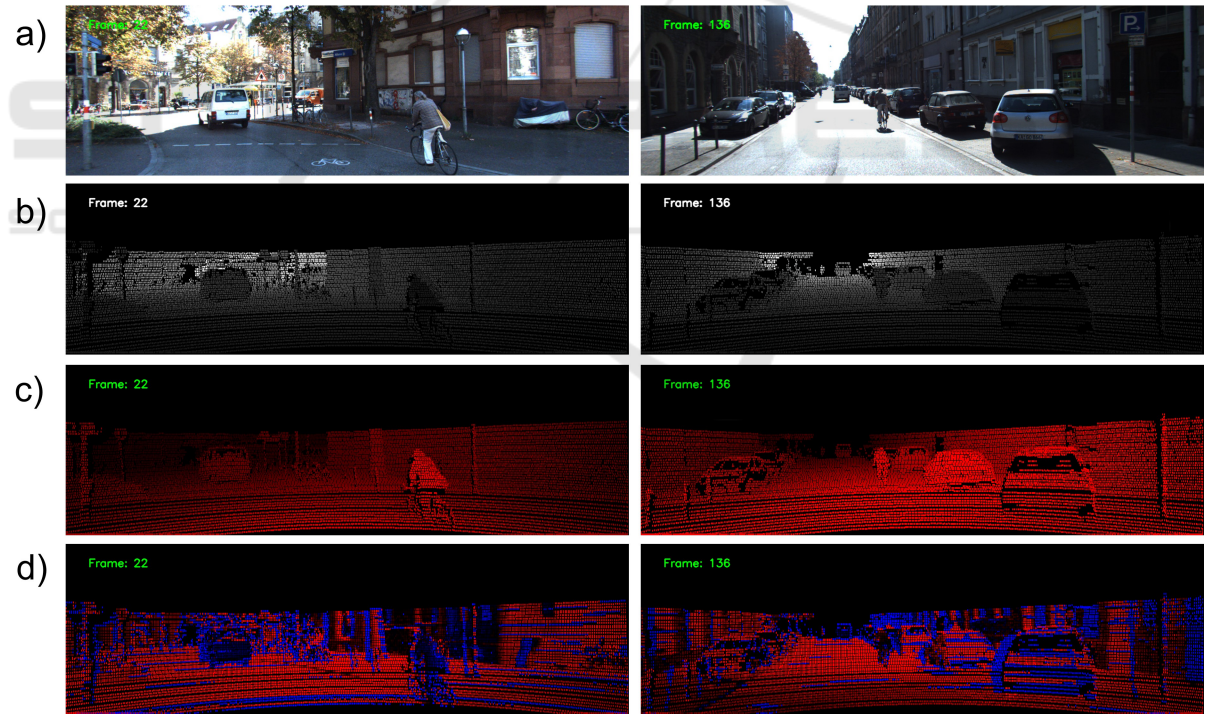

Figure 10: Looming from Lidar: a) Original image, b) Depth from LiDAR, c) Looming from LiDAR + IMU, d) Estimated looming from LiDAR only.

of view of the color camera. Also shown are top and bird's eye views of the data for a specific time instant of the video.

4.3 Estimation of Looming using LiDAR

In Figure 8, original images from two consecutive frames (frames 22 and 23) are shown along LiDAR

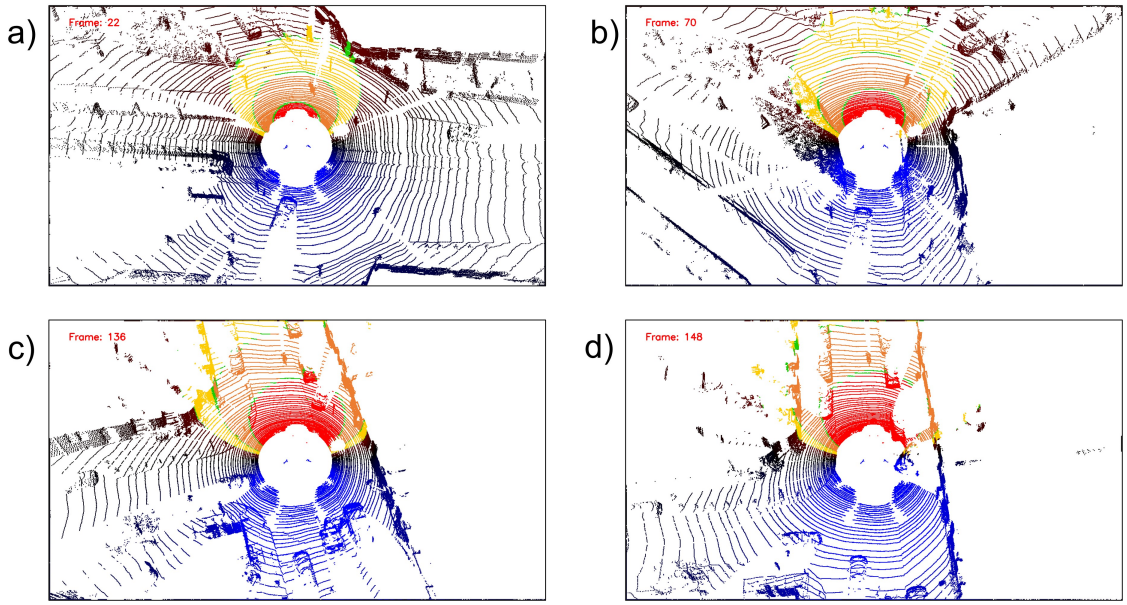

Figure 11: Threat zones expanding and contracting according to looming (refer to text for details).

views (360 degrees) for two time instants. The resultant looming estimation using equation (5) is also shown at the bottom of Figure 8. Notice positive values of looming are shown in red and corresponds mainly to points along the forward direction of motion (around the center of the image).

Due to the effect of occlusions of points, there are sudden changes in range between frames, causing an "edge-effect" around objects with incorrect looming values, shown in intense red or blue colors. *However an important advantage is that the method incorporates values of looming as obtained from moving objects.* For example, the bicycle in the middle of the image is correctly portrayed with dark colors, meaning low values of looming as expected for this kind of motion since the bicycle velocity almost matches the velocity of the vehicle, and the rate of change in range is close to zero.

4.4 Looming from LiDAR and IMU

We use equation (4) to compute looming for each point. From the IMU sensor we obtained the translation velocity vector $\mathbf{t}$ and from the LiDAR sensor we obtained the range r. Figure 9 shows top and bird's eye views for two time instants. Color intensity was assigned to each point representing the obtained looming value: red for positive values, and blue for negative values.

We can see that the looming is very similar to the expected shown in simulation. *This method adequately registers looming for stationary objects; however, it is imprecise for moving objects since the relative speed is not considered.*

In Figure 10 a comparison between both methods is shown.

4.5 Threat Zones for Collision Free Navigation

In Figure 11 several threat zones are computed using looming from section 4.4: *red zone* - high threat, *orange zone* - medium threat and *yellow zone* - low threat. Notice how the threat zones change sizes between frames, this is due to the change in speed of the vehicle.

5 CONCLUSIONS

In this paper we demonstrate how to compute looming *directly* from raw LiDAR data without 3D reconstruction. There is no need for scene understanding such as identifying cars, bikes, or pedestrians. Two approaches are shown, one uses LiDAR data only, and the other uses LiDAR data combined with IMU.

The approach shows that looming provides information about imminent threat that can potentially be used for navigation tasks such as obstacle avoidance. The paper shares highly encouraging initial results and should be considered as "work in progress" as more looming from LiDAR-related methods are being explored.

ACKNOWLEDGEMENTS

The authors thank Dr. Sridhar Kundur for many fruitful discussion and suggestions that led to meaningful improvements of this manuscript.

REFERENCES

Ache, J. M., Polsky, J., Alghailani, S., Parekh, R., Breads, P., Peek, M. Y., Bock, D. D., von Reyn, C. R., and Card, G. M. (2019). Neural basis for looming size and velocity encoding in the drosophila giant fiber escape pathway. *Current Biology*, 29(6):1073–1081.

Albus, J. S. and Hong, T. H. (1990). Motion, depth, and image flow. In *Proceedings., IEEE International Conference on Robotics and Automation*, pages 1161–1170. IEEE.

Aloimonos, Y. (1992). Is visual reconstruction necessary? obstacle avoidance without passive ranging. *Journal of Robotic Systems*, 9(6):843–858.

Evans, D. A., Stempel, A. V., Vale, R., Ruehle, S., Lefler, Y., and Branco, T. (2018). A synaptic threshold mechanism for computing escape decisions. *Nature*, 558(7711):590–594.

Geiger, A., Lenz, P., Stiller, C., and Urtasun, R. (2013). Vision meets robotics: The kitti dataset. *The International Journal of Robotics Research*, 32(11):1231–1237.

Grigorescu, S., Trasnea, B., Cocias, T., and Macesanu, G. (2020). A survey of deep learning techniques for autonomous driving. *Journal of Field Robotics*, 37(3):362–386.

Kundur, S. R. and Raviv, D. (1999). Novel active vision-based visual threat cue for autonomous navigation tasks. *Computer Vision and Image Understanding*, 73(2):169–182.

Mujumdar, A. and Padhi, R. (2011). Evolving philosophies on autonomous obstacle/collision avoidance of unmanned aerial vehicles. *Journal of Aerospace Computing, Information, and Communication*, 8(2):17–41.

Raviv, D. (1992). *A quantitative approach to looming*. US Department of Commerce, National Institute of Standards and Technology.

Raviv, D. and Joarder, K. (2000). The visual looming navigation cue: A unified approach. *Comput. Vis. Image Underst.*, 79:331–363.

Ridwan, I. (2018). *Looming object detection with event-based cameras*. University of Lethbridge (Canada).

Roriz, R., Cabral, J., and Gomes, T. (2021). Automotive lidar technology: A survey. *IEEE Transactions on Intelligent Transportation Systems*.

Sharma, O., Sahoo, N. C., and Puhan, N. (2021). Recent advances in motion and behavior planning techniques for software architecture of autonomous vehicles: A state-of-the-art survey. *Engineering applications of artificial intelligence*, 101:104211.

Wang, M., Voos, H., and Su, D. (2018). Robust online obstacle detection and tracking for collision-free navigation of multirotor uavs in complex environments. In *2018 15th International Conference on Control, Automation, Robotics and Vision (ICARCV)*, pages 1228–1234. IEEE.

Yasin, J. N., Mohamed, S. A., Haghbayan, M.-H., Heikkonen, J., Tenhunen, H., and Plosila, J. (2020). Unmanned aerial vehicles (uavs): Collision avoidance systems and approaches. *IEEE access*, 8:105139–105155.

Zhang, J. and Singh, S. (2014). Loam: Lidar odometry and mapping in real-time. In *Robotics: Science and Systems*, volume 2, pages 1–9. Berkeley, CA.